Fano resonances due to coupled magnetoexciton and continuum states in bulk semiconductors

S. Glutsch, U. Siegner, M.-A. Mycek, and D. S. Chemla
Department of Physics, University of California at Berkeley, Berkeley, California 94720
and Materials Sciences Division, Lawrence Berkeley Laboratory, Berkeley, California 94720
(Received 8 June 1994; revised manuscript received 20 July 1994)

We have observed Fano resonances in linear absorption experiments on GaAs under a magnetic field. In a bulk semiconductor in a magnetic field, Fano interference is the result of the coupling of higher-order magnetoexcitons and energetically degenerate one-dimensional continuum states. We show that these experimental findings can be described by the model of a two-band semiconductor in the effective-mass approximation. Numerical calculations of the linear magnetoabsorption are presented that demonstrate that the coupling between magnetoexcitons and continuum states is due to Coulomb interaction.

I. INTRODUCTION

Fano interference is the result of the quantum mechanical coupling between a discrete state and an energetically degenerate continuum of states.[1] If optical transitions from a common ground state to both the discrete state and the continuum are allowed, Fano interference manifests itself in the optical absorption spectrum by an asymmetric line shape, the so-called Fano-Beutler profile. This profile has a pronounced minimum at the energy where the interference between the transition amplitudes of the discrete state and the continuum is destructive.

Fano interference has been widely discussed in atomic physics in the context of autoionizing states, which are found in a variety of atomic systems.[2] In semiconductor physics, only a few examples of Fano interference have been reported so far from interband absorption experiments. The energy spectrum of intrinsic semiconductors is comprised of continuum band states and discrete exciton states. Since excitons are the lowest lying optical excitations in intrinsic bulk semiconductors, they do not energetically overlap with continuum band states. Fano interference between excitons and band states is not possible in this situation. Consequently, the reported experimental observations and theoretical predictions of Fano interference in semiconductors involve heterostructures,[3–6] doped semiconductors[7] or biexciton resonances.[8] In these cases, overlapping discrete and continuum states are found.

In this paper, we demonstrate a concept for the creation of Fano resonances in intrinsic bulk semiconductors involving excitons and band states. The application of a magnetic field to a semiconductor leads to the formation of Landau levels in the valence and in the conduction band. Importantly, the field only quantizes states with the wave vector perpendicular to the direction of the field. States with the wave vector parallel to the field form one-dimensional continua corresponding to each Landau level. Taking into account Coulomb interaction, it is found that magnetoexcitons are formed corresponding to each pair of valence band and conduction band Landau levels with the same Landau quantum number.[9] Since the discrete higher-order magnetoexcitons overlap in energy with continua belonging to lower-order Landau levels, Fano interference between them can be expected.

Although the magneto-optical absorption in GaAs has been studied carefully in terms of resonance positions and selection rules,[10–12] the question of Fano interference has not been addressed so far in the context of magnetoexcitons in bulk semiconductors. To the best of our knowledge, the only experimental evidence for Fano interference in this situation has been reported in Ref. 13. Here, we present the first comprehensive experimental and theoretical study of Fano interference between magnetoexcitons and continuum states in a bulk semiconductor. We like to point out that Fano interference cannot be observed in magneto-optical experiments on two-dimensional quantum well structures since in quantum wells the necessary continuum states have been removed by the layered structure. Magneto-optical experiments are, therefore, an important example for qualitatively different physics due to a change of the dimensionality of a semiconductor.

The paper is organized as follows. In Sec. II, we describe the experimental setup for magnetoabsorption experiments and discuss the experimental results obtained on a high-quality GaAs bulk sample. These experiments show that under magnetic field pronounced Fano resonances are formed in GaAs, which can be traced back to the underlying magnetoexciton states. The theoretical model which accounts for the experimental findings is presented in Sec. III. This model demonstrates that the coupling which gives rise to Fano interference is due to Coulomb interaction. In Sec. IV, we summarize our results.

II. EXPERIMENT

Experiments have been performed on a high-quality bulk GaAs sample of a thickness of 1 μm. The sample was

0163-1829/94/50(23)/17009(9)/$06.00

grown on a GaAs substrate by molecular beam epitaxy. In order to allow transmission experiments, the substrate was removed by chemical etching and the sample was glued on a sapphire substrate. Both sides of the sample have been antireflection coated.

The sample was put in a split-coil magnet in which the magnetic field can be varied between 0 and 12 T. The field was applied along the growth direction of the sample and parallel to the propagation vector of the excitation light. In all experiments, the sample was held at a temperature of 1.6 K.

Transmission spectra have been measured with a white light source and a 25 cm spectrometer equipped with an optical multichannel analyzer. This setup provides an overall energy resolution of 0.25 meV in the relevant wavelength range. All absorption spectra have been corrected for the spectral transmission characteristics of the optical setup.

We have measured absorption spectra with right-handed or left-handed circularly polarized light in order to excite pure spin states. Distinct Fano resonances have been observed for both circular polarizations. The main difference between σ^- and σ^+ absorption spectra is the absolute energy of the resonances. In Ref. 10, it has been shown that this difference is the result of different optical selection rules for transitions between valence band and conduction band Landau levels excited with σ^- and σ^+ circularly polarized light. Since the absolute resonance energy is of minor importance in the context of Fano interference, we will concentrate on the experimental results obtained under σ^- excitation.

Figure 1 depicts linear absorption spectra for magnetic fields $B = 0$, 2, 6, and 12 T. The zero-field spectrum shows that the light-hole (lh) and heavy-hole (hh) exciton transitions are split in this sample. The splitting is due to mechanical strain,[14] which results from different thermal expansion coefficients of the GaAs layer and the sapphire substrate on which the GaAs sample is mounted. Mechanical strain shifts the lh valence band and the hh valence band to lower energies where the shift of the lh band is larger.[14] Consequently, the degeneracy between the two bands at the center of the Brillouin zone is lifted and the corresponding exciton transitions are split. The full width at half maximum of the hh and lh absorption line at zero field is 1.3 meV and 0.9 meV, respectively. These very small linewidths show the high quality of the sample in which inhomogeneous broadening of the optical transitions can be neglected. Due to the small energy separation between the maximum and the minimum of a Fano resonance, inhomogeneous broadening prevents the observation of Fano interference and is most likely the reason that Fano resonances have not been observed in other magnetoabsorption experiments on bulk semiconductors.[15,16]

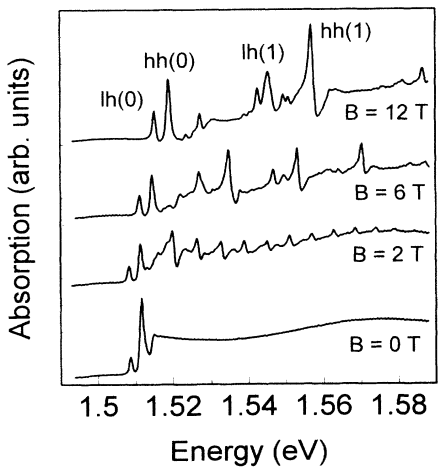

FIG. 1. Experimental linear absorption spectra of bulk GaAs for different magnetic fields between 0 and 12 T. All spectra have been measured with σ^- circularly polarized light at a temperature of 1.6 K. The Lorentzian light-hole and heavy-hole resonances are labeled lh(0) and hh(0), respectively. Fano resonances are labeled hh(n) and lh(n) with Landau quantum number $n \geq 1$.

In our high-quality sample, if a magnetic field is applied, already at fields as low as 2 T structures appear in the continuum. With increasing field, the modulation amplitude of the structures becomes larger and the energy splitting between adjacent resonances increases. These structures turn out to be Fano resonances. Importantly, the asymmetric resonances show minima *below* the continuum absorption, demonstration that *interference* between discrete magnetoexcitons and continuum states takes place due to coupling.

Here, it has to be taken into account that all hh and lh magnetoexciton scattering states below a certain energy contribute to different continua at this energy. Since several continua are involved in the formation of the Fano resonances, the absorption minimum is finite,[1] whereas in the simplest case of one discrete state coupled to one continuum the absorption drops to zero if homogeneous broadening is neglected.[1] The height of the relevant continuum for a certain resonance is roughly given by the height of the continuum absorption directly at the low-energy onset of the resonance. Without coupling, the magnetoexciton absorption would simply add to the continuum absorption and reduction of the overall absorption below this continuum level would not be observed. Thus, these data provide clear evidence for Fano interference. At a field of 6 T distinct Fano profiles are observable. They become even more pronounced if the field is further increased to $B = 12$ T.

In order to unambiguously demonstrate that the asymmetric profiles which we observe in the continuum part of the absorption spectra are Fano resonances, we apply Fano's theory[1] to fit the experimental data.

The absorption profile α of a Fano resonance has the form[1]

$$\alpha \propto \frac{(\epsilon - q)^2}{1 + \epsilon^2} .$$

In this expression, ϵ is a normalized energy which is given by $\epsilon = (\Omega - E)/\Gamma$ where Ω is the resonance energy of the discrete state and Γ describes the strength of the coupling between the discrete state and the continuum states. Γ is

related to the coupling matrix element V by $\Gamma = \pi|V|^2$. The parameter q gives the ratio of the optical transition matrix elements for the transitions to the discrete state and the continuum.

The parameters Ω, Γ, and q which determine the Fano profile can be obtained from a simple analysis of the experimental absorption line. This analysis uses the energies of the absorption maximum and minimum as well as the full width at half maximum of the Fano line as input. As an example, we have deduced the Fano parameters for one of the resonances observed at a field of 10 T and calculated the Fano profile from the parameters.

In the lower part of Fig. 2, we show the experimental absorption spectrum at a field $B = 10\,\mathrm{T}$. The pronounced Fano resonance in the dashed box stems from the heavy-hole magnetoexciton corresponding to the second ($n = 1$) Landau transition, as will be shown below. The upper part of Fig. 2 depicts a close-up of this Fano resonance. The experimental data are marked by the squares. The Fano parameters we have obtained analyzing this resonance are $\Omega = 1549.5\,\mathrm{meV}$, $\Gamma = 0.668\,\mathrm{meV}$, and $q = -2.86$. The Fano profile calculated from these parameters is plotted in the upper part of Fig. 2 as a solid line. The agreement with the experimentally determined Fano profile is good, demonstrating that the observed asymmetric absorption lines are indeed the result of Fano interference. The small deviation at the high-energy side of the Fano line is due to the contribution of the $2s$ magnetoexciton state, which, of course, is not included in this single-resonance Fano model.

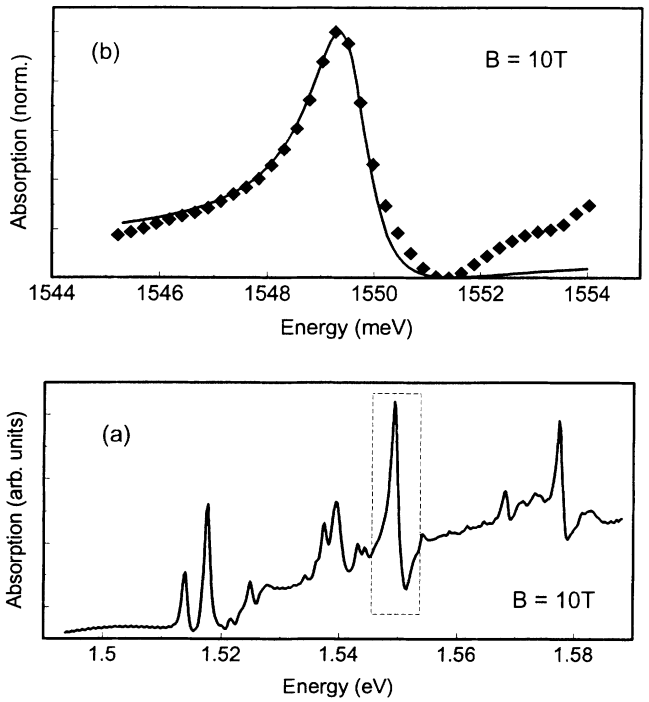

FIG. 2. (a) Low-temperature absorption spectrum of GaAs for a magnetic field $B = 10$ T. The Fano resonance in the dashed box originates from the heavy-hole magnetoexciton corresponding to the second Landau transition. (b) The squares show a close-up of the experimentally observed Fano profile marked in (a) by the dashed box. The solid line is a fit to the experimental data using the expression for the absorption line shape which describes Fano interference. The parameters are given in the text.

The Fano profiles originate from the coupling of discrete higher-order magnetoexcitons to one-dimensional continua belonging to lower-order Landau levels. Here, higher-order magnetoexcitons refers to magnetoexcitons which correspond to the second (n=1), third, etc., pair of valence and conduction band Landau levels with the same Landau quantum number. It should be noted that every magnetoexciton transition, in principle, consists of a complete Rydberg series, where, however, the excited magnetoexciton states are barely resolvable in the experimental spectrum. The absorption spectra depicted in Figs. 1 and 2 also demonstrate that the lowest-order lh and hh magnetoexcitons corresponding to the first (n=0) pair of Landau levels do not form Fano resonances. These resonances exhibit Lorentzian absorption profiles in sharp contrast with the profile of the higher-energy resonances. The lowest-order lh magnetoexciton is the lowest resonance in the spectrum and thus is not degenerate to continuum states. It is worth noting that the lowest-order hh magnetoexciton cannot couple to continuum states either, since the splitting between the lh exciton and the hh exciton is too small to bring the hh exciton in resonance with lh continuum states. The lh–hh splitting varies between 2.9 meV at zero field and 3.7 meV at $B = 12$ T, i.e., the splitting is smaller than the excitonic Rydberg for all relevant fields.

Since the degeneracy between the hh and lh valence bands has been lifted, the spectra at finite magnetic fields show two series of Fano resonances, corresponding to hh and lh magnetoexcitons. Each discrete state, i.e., each hh or lh magnetoexciton, gives rise to one Fano resonance, in the formation of which, however, several continua can be involved, as discussed above. The superposition of two series of Fano resonances is the reason for the complicated form of the spectra.

In order to distinguish between lh and hh Fano resonances more clearly, the resonance energies of the different spectral feature are plotted as a function of the magnetic field in Fig. 3. Figure 3 shows the magnetic field dependence of the lowest-order Lorentzian magnetoexcitons and the first and second Fano resonances of the light hole (asterisks, dashed lines) and the heavy hole (squares, solid lines), respectively. While the lowest-order magnetoexcitons only exhibit a slight diamagnetic shift with increasing field, the magnetic field dependence of the Fano resonance energies is linear. This linear field dependence of Fano resonance energies is expected since the transition energy is essentially given by the energy of the corresponding pair of Landau levels.

The fan charts shown in Fig. 3 allow verification of the assignment of the different Fano resonances to hh and lh transitions. For this purpose, we have calculated the effective masses of the excitons underlying the Fano states and compared them to the values which can be calculated from literature data. Taking into account that the hole quantizes with the mass in the direction perpendicular to

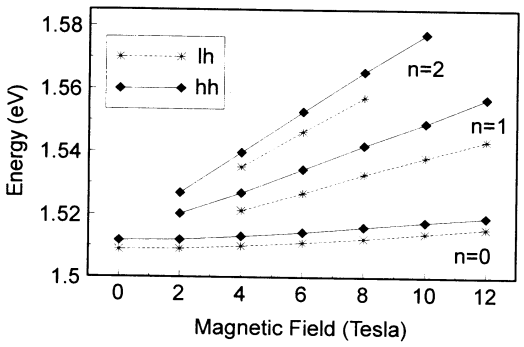

FIG. 3. Resonance energies of the lowest-order ($n = 0$) light-hole and heavy-hole magnetoexcitons and the first ($n = 1$) and second ($n = 2$) light-hole and heavy-hole Fano resonances as a function of the magnetic field. Light-hole transitions: asterisks; heavy-hole transitions: squares.

the magnetic field and using the values for the effective electron mass and the Luttinger parameters from Ref. 17, we find $m_{\mathrm{hh}} = 0.112\,m_0$ for the effective mass of the heavy hole, i.e., the state with the angular momentum $\pm\,{}^3/_2$, and $m_{\mathrm{hh}}^{(\mathrm{Ex})} = 0.042\,m_0$ for the mass of the heavy-hole exciton, where m_0 is the bare electron mass. For the mass of the light hole, i.e., the state with the angular momentum $\pm\,{}^1/_2$, we obtain a value of $m_{\mathrm{lh}} = 0.211\,m_0$ from the literature data and a corresponding light-hole exciton mass of $m_{\mathrm{lh}}^{(\mathrm{Ex})} = 0.052\,m_0$.

Using a simple model in which the cyclotron energy $\hbar\omega_{\mathrm{c}}$ of the magnetoexciton is given by $\hbar\omega_{\mathrm{c}} = \hbar eB/m^{(\mathrm{Ex})}$, we deduced a heavy-hole exciton mass $m_{\mathrm{hh}}^{(\mathrm{Ex})} = 0.032\,m_0$ and a light-hole exciton mass $m_{\mathrm{lh}}^{(\mathrm{Ex})} = 0.042\,m_0$ from the experimental fan charts. The agreement with the literature values is reasonable. Thus, the fan charts plotted in Fig. 3 confirm the assignment of the different Fano resonances to the underlying lh and hh magnetoexciton transitions.

Summarizing the experimental findings, we have observed pronounced Fano resonances in the linear absorption spectra of bulk GaAs under magnetic field. The experimental data can be well described by the model for a discrete state coupled to a continuum which has been introduced by Fano.[1] The magnetic field dependence of the Fano resonance energies allows us to trace back the Fano profiles to the underlying heavy-hole and light-hole magnetoexcitons.

III. THEORY

In the theory part of this paper, we show that the experimental observation of Fano interference due to coupled magnetoexcitons and continuum states in bulk GaAs can be accounted for by the model of a two-band semiconductor in the effective-mass approximation. For this purpose, we have calculated the linear absorption spectrum for a two-band isotropic semiconductor in a constant magnetic field. The Coulomb term has been included in the calculation. While the influence of a magnetic field on the optical absorption of excitons in the idealized pure two-dimensional systems is well known,[18] the three-dimensional problem has not been completely solved so far. Our theoretical results not only reproduce the experimental observation of Fano interference but also give evidence of the nature of the coupling between magnetoexcitons and continuum states. We will demonstrate that the coupling is the result of Coulomb interaction.

We start with a very general Green's function description of a semiconductor in an electromagnetic field and derive the two-particle Schrödinger equation for an electron and a hole in a magnetic field including the Coulomb term and obtain a generalized Elliott formula[19] for the linear susceptibility. The two-particle Schrödinger equation is a partial differential equation with six variables and is extremely difficult to solve, in particular, when continuum states are involved. Therefore, we show how the relative motion of the electron and hole and the center-of-mass motion can be separated. Moreover, we demonstrate that the optical absorption spectrum of a semiconductor in a magnetic field solely depends on the relative coordinate between the Coulomb bound electron and hole. After the separation of the relative and center-of-mass motion, we obtain the Schrödinger equation for the relative motion, which has only two spatial variables (perpendicular and parallel to the magnetic field) and can be solved numerically. The linear absorption spectrum can then be calculated from the eigenfunctions using the generalized Elliott formula. At the end of the theoretical part of the paper, we present and discuss the results of the numerical calculations.

In order to describe the experimental facts theoretically, we introduce a model of a two-band semiconductor in a magnetic field. The Coulomb potential, which is essential to describe the Fano resonances, is treated in the Hartree-Fock approximation. The light-matter interaction is described by dipole coupling. In this respect, the density matrix n is the central quantity of the theory. It allows us to calculate the polarization according to

$$P(t) = \frac{1}{\Omega}\,\mathrm{Tr}\left[\,\mu\, n(t)\,\right], \tag{1}$$

where μ is the dipole operator and Ω the normalization volume. In the frequency domain, the first-order polarization is given by $P(\omega) = \varepsilon_0\,\chi(\omega)\,E(\omega)$, where E is the field strength of the incoming light field, and χ is the linear optical susceptibility. The imaginary part of χ describes the optical absorption. The density matrix n is related to the Green's function by

$$n_{ij}(\mathbf{r}_1,\mathbf{r}_2,t) = i\hbar\, G_-{}^{+}{}_{ij}(\mathbf{r}_1,\mathbf{r}_2,t,t)\,. \tag{2}$$

Since there are well-known techniques to calculate G, we focus first on the Green's function and deduce later an equation for density matrix n.

Within the standard treatment of Bloch electrons in a magnetic field,[20] the inverse Green's function can be written as

$$G^{-1}{}_A{}^B{}_{ij}(\mathbf{r}_1,\mathbf{r}_2,t_1,t_2) = G^{(0)-1}{}_A{}^B{}_{ij}(\mathbf{r}_1,\mathbf{r}_2,t_1,t_2) - \Sigma_A{}^B{}_{ij}(\mathbf{r}_1,\mathbf{r}_2,t_1,t_2)\,, \quad (3)$$

where

$$G^{(0)-1}{}_A{}^B{}_{ij}(\mathbf{r}_1,\mathbf{r}_2,t_1,t_2) = \left[i\hbar\frac{\partial}{\partial t_1} - \frac{1}{2m_i}\left|\frac{\hbar}{i}\nabla_1 + e\,\mathbf{A}(\mathbf{r}_1,t_1)\right|^2 + e\,U(\mathbf{r}_1,t_1)\right] \times \delta_A^B\,\delta_{ij}\,\delta(\mathbf{r}_1-\mathbf{r}_2)\,\delta(t_1-t_2)\,.$$

Here, m_i is the effective mass of an electron in the band i, $-e$ the electron charge, and $\mathbf{A}$ and U represent the vector and scalar potential of the electromagnetic field, respectively. The indices A and B denote the branches of the Keldysh contour and $\Sigma_A{}^B{}_{ij}(\mathbf{r}_1,\mathbf{r}_2,t_1,t_2)$ is the self-energy. Without loss of generality, the band edges are set to zero resulting in a shift of the optical spectra by the gap energy. In fact, $G^{(0)-1}$ is singular as an operator so that G is not uniquely determined by $G^{(0)-1}$. It is sufficient, however, to have an initial condition $n_{ij}(\mathbf{r}_1,\mathbf{r}_2,t_0) = n_{ij}^{(0)}(\mathbf{r}_1,\mathbf{r}_2)$ for the density matrix (2).

Now, we focus on a two-band semiconductor (i,j = c, v) in a stationary magnetic field $\mathbf{A}(\mathbf{r})$. The Hartree-Fock approximation yields for the self-energy:

$$\Sigma_A{}^B{}_{ij}(\mathbf{r}_1,\mathbf{r}_2,t_1,t_2) = -V(\mathbf{r}_1,\mathbf{r}_2)\left[n_{ij}(\mathbf{r}_1,\mathbf{r}_2,t_1) - n_{ij}^{(0)}(\mathbf{r}_1,\mathbf{r}_2)\right]\delta_A^B\,\delta(t_1-t_2)\,, \quad (4)$$

where $V(\mathbf{r}_1,\mathbf{r}_2)$ is the Coulomb potential screened by the background dielectric constant ε. Assuming a light-matter coupling by a dipole matrix element $\mu_{cv} = \mu_{vc}^*$ only, from Eq. (2) the equation of motion for the off-diagonal elements of the density matrix n can be derived, leading to

$$i\hbar\frac{\partial}{\partial t}\,n_{cv}(\mathbf{r}_1,\mathbf{r}_2,t) = \left[\frac{1}{2m_c}\left|+\frac{\hbar}{i}\nabla_1 + e\,\mathbf{A}(\mathbf{r}_1)\right|^2 - \frac{1}{2m_v}\left|-\frac{\hbar}{i}\nabla_2 + e\,\mathbf{A}(\mathbf{r}_2)\right|^2 - V(\mathbf{r}_1,\mathbf{r}_2)\right] \times n_{cv}(\mathbf{r}_1,\mathbf{r}_2,t) - \mu_{cv}\,\delta(\mathbf{r}_1-\mathbf{r}_2)E(t)\left[n_{vv}(\mathbf{r}_1,\mathbf{r}_2,t) - n_{cc}(\mathbf{r}_1,\mathbf{r}_2,t)\right]. \quad (5)$$

The semiconductor is assumed to be at zero temperature, i.e., the density matrix before excitation is $n^{(0)}(\mathbf{r}_1,\mathbf{r}_2) = \mathrm{diag}(0,1)\,\delta(\mathbf{r}_1-\mathbf{r}_2)$. Within the two-band model, the polarization field (1) is then given by the explicit expression

$$P(t) = \frac{1}{\Omega}\int_\Omega d^3\mathbf{r}\left[\mu_{cv}\,n_{vc}(\mathbf{r},\mathbf{r},t) + \mu_{vc}\,n_{cv}(\mathbf{r},\mathbf{r},t)\right]. \quad (6)$$

In order to obtain the linear optical susceptibility, we introduce the Fourier transforms of E

$$E(\omega) = \int_{-\infty}^{+\infty} dt\,e^{i\omega t}\,E(t),$$

and P, respectively. Taking the Fourier transform of the differential equation (5), we find for the linear optical susceptibility,

$$\chi(\omega) = -\frac{|\mu|^2}{\varepsilon_0}\frac{1}{\Omega}\int_\Omega d^3\mathbf{r}\int_\Omega d^3\mathbf{r}' \times\sum_\Lambda \frac{\Phi^{(\Lambda)}(\mathbf{r},\mathbf{r})\,\Phi^{(\Lambda)*}(\mathbf{r}',\mathbf{r}')}{E^{(\Lambda)} - \hbar(\omega+i\eta)}\,. \quad (7)$$

Here, the abbreviation $\mu = \mu_{cv}$ is used. The quantity $\eta = +0$ is introduced to obtain the physically relevant retarded solution of Eq. (5). In practice, it represents the homogeneous linewidth. The functions $\Phi^{(\Lambda)}$ are solutions of the two-particle Schrödinger equation,

$$\left[\frac{1}{2m_e}\left|\frac{\hbar}{i}\nabla_e + e\,\mathbf{A}(\mathbf{r}_e)\right|^2 + \frac{1}{2m_h}\left|\frac{\hbar}{i}\nabla_h - e\,\mathbf{A}(\mathbf{r}_h)\right|^2 - \frac{e^2}{4\pi\varepsilon_0\varepsilon|\mathbf{r}_e-\mathbf{r}_h|}\right]\Phi^{(\Lambda)}(\mathbf{r}_e,\mathbf{r}_h) = E^{(\Lambda)}\,\Phi^{(\Lambda)}(\mathbf{r}_e,\mathbf{r}_h)\,, \quad (8)$$

which describes the motion of an electron and hole with masses $m_e = m_c > 0$ and $m_h = -m_v > 0$ in a magnetic field. Equation (7) can be looked upon as a generalization of the well known Elliott formula.[19]

The two-particle Schrödinger equation (8) and the generalized Elliott formula (7) accurately describe the physics, but are not useful for practical purposes since they cannot be solved explicitly. Therefore, in the following we show how the relative motion of the electron and hole and the center-of-mass motion can be separated. This treatment yields a Schrödinger equation for the relative coordinate and a corresponding Elliott formula, which can be solved numerically.

We assume that the magnetic field $\mathbf{B} = B_z\,\mathbf{e}_z$ is homogeneous in the semiconductor. Thus, a semiconductor in this magnetic field is a spatially homogeneous system, i.e., the macroscopic properties of this system do not depend on the spatial position. Difficulties, however, arise from the form of the vector potential. Any vector po-

tential $\mathbf{A}$ with the property $\nabla \times \mathbf{A}(\mathbf{r}) \equiv \mathbf{B}$ depends on the spatial coordinate and it is not obvious how the separation of the relative and the center-of-mass motion can be achieved. This problem has been solved by Gor'kov and Dzyaloshinskii.[21] Their method has been successfully applied to the two-dimensional magnetoexciton.[22]

We give a brief outline of this method.[21] If we consider the differential operator in Eq. (8) as a representation of a two-particle Hamiltonian $\hat{H}$ and use the gauge $\mathbf{A}(\mathbf{r}) = \frac{1}{2}\mathbf{B} \times \mathbf{r}$, we find that the equations $[\hat{\mathbf{Q}}, \hat{H}] = \mathbf{0}$ and $\hat{\mathbf{Q}} \times \hat{\mathbf{Q}} = \mathbf{0}$ hold for the operator $\hat{\mathbf{Q}} = \hat{\mathbf{p}}_e + \hat{\mathbf{p}}_h - \frac{1}{2} e\,\mathbf{B} \times (\hat{\mathbf{r}}_e - \hat{\mathbf{r}}_h)$. Therefore, $\hat{\mathbf{Q}}$ is a constant of motion, and Eq. (8) becomes separable. Since only wave functions with zero center-of-mass wave vector and zero relative angular momentum have to be considered for optically allowed transitions, the optical susceptibility (7) becomes

$$\chi(\omega) = -\frac{|\mu|^2}{\varepsilon_0} \sum_{\lambda} \frac{|\varphi^{(\lambda)}(0,0)|^2}{E^{(\lambda)} - \hbar(\omega + i\eta)} , \tag{9}$$

where the $\varphi^{(\lambda)}$ and $E^{(\lambda)}$ are solutions of

$$\left\{ -\frac{\hbar^2}{2m}\left[\frac{1}{\rho}\frac{\partial}{\partial\rho}\left(\rho\frac{\partial}{\partial\rho}\right) + \frac{\partial^2}{\partial\zeta^2}\right] + \frac{m}{8}\omega_c^2\rho^2 - \frac{e^2}{4\pi\varepsilon_0\varepsilon\sqrt{\rho^2+\zeta^2}} \right\} \varphi^{(\lambda)}(\rho,\zeta) = E^{(\lambda)}\varphi^{(\lambda)}(\rho,\zeta) \tag{10}$$

with the reduced exciton mass m and the cyclotron frequency $\omega_c = \sqrt{e^2 B_z^2/m^2}$. ρ and ζ are cylindrical coordinates which refer to the relative motion of the electron and hole.

Thus, after the separation of the center-of-mass motion, we have obtained a Schrödinger equation (10) which depends only on two variables. This equation can be solved numerically, and the optical spectrum can be computed from Eq. (9).

Importantly, Eq. (9) shows that the optical absorption spectrum is solely determined by the relative motion of the electron and the hole and, therefore, by the reduced mass m of the exciton. We emphasize that this result does not necessarily follow from the spatial homogeneity that is evident from the physical circumstances. In fact, the third-order polarization depends on the separate motion of electrons and holes. This will be discussed in more detail in a forthcoming publication.

Though the optical susceptibility of a geometrically confined one-dimensional microstructure can be described by a formula of the same type as Eq. (7), no further reduction is possible to equations of the same type as Eqs. (9) and (10). Thus, the linear spectrum of a microstructure is affected by the center-of-mass motion,[23,24] in contrast to the case of a three-dimensional semiconductor in a magnetic field. Consequently, the analogy of magnetic and structural confinement should not be overemphasized. A bulk semiconductor in a magnetic field shows an even better one-dimensional behavior than a geometrically confined one-dimensional structure.

In order to check whether the model of a two-band semiconductor in a magnetic field can account for the experimental observation of Fano interference involving magnetoexcitons and one-dimensional continuum states in GaAs, we now investigate Eq. (10). First, we analyze how Fano resonances are formed. For this purpose, we expand the partial differential equation (10) in the radial eigenfunctions ψ_n of a two-dimensional harmonic oscillator with eigenenergies E_n according to

$$\varphi^{(\lambda)}(\rho,\zeta) = \sum_{n=0}^{\infty} f_n^{(\lambda)}(\zeta)\,\psi_n(\rho) ,$$

$$\left[-\frac{\hbar^2}{2m}\left(\frac{1}{\rho}\frac{d}{d\rho}\rho\frac{d}{d\rho}\right) + \frac{m}{8}\omega_c^2\rho^2 \right] \psi_n(\rho) = E_n\,\psi_n(\rho) ,$$

The ψ_n describe the motion in the xy plane. Then we obtain

$$\sum_{n'}\left[\left(-\frac{\hbar^2}{2m}\frac{d^2}{d\zeta^2} + E_n\right)\delta_{nn'} - V_{nn'}(\zeta)\right] f_{n'}^{(\lambda)}(\zeta) = E^{(\lambda)} f_n^{(\lambda)}(\zeta) ,$$

$$V_{nn'}(\zeta) = 2\pi\int_0^{\infty} d\rho\,\rho\,\psi_n^*(\rho)\,\psi_{n'}(\rho)\,\frac{e^2}{4\pi\varepsilon_0\varepsilon\sqrt{\rho^2+\zeta^2}} . \tag{11}$$

Here, $V_{nn'}$ is the Coulomb matrix element, still depending on the coordinate ζ. These equations represent a coupled set of ordinary differential equations. It is interesting to compare the three-dimensional case to the case of a quantum well in a magnetic field.[18]

In the quantum well case, the coordinate ζ is absent and a purely discrete energy spectrum is obtained for any field $B > 0$. The transition from a two-dimensional system to a three-dimensional one produces an additional feature: Due to the unrestricted motion in the z direction described by the coordinate ζ, excitons *and* continuum states are formed corresponding to each Landau level. Since the different Landau levels are separated by the energy $\hbar\omega_c$, excitons belonging to higher-order Landau levels are degenerate with continuum states of the lower ones. These states interfere because of the existence of the off-diagonal Coulomb potentials $V_{nn'}$ $(n \neq n')$. For such a pair of energetically degenerate discrete and continuum states $|n,\alpha\rangle$ and $|n',E\rangle$ with Landau quantum numbers $n \neq n'$ and energies $E_{n\alpha} = E$, the Fano coupling V_E (Ref. 1) is given by

$$V_E = -2\pi\int_0^{\infty} d\rho\,\rho\int_{-\infty}^{+\infty} d\zeta\,\psi_n^*(\rho)\,\phi_{n\alpha}^*(\zeta)\,\frac{e^2}{4\pi\varepsilon_0\varepsilon\sqrt{\rho^2+\zeta^2}} \times \phi_{n'E}(\zeta)\,\psi_{n'}(\rho) , \tag{12}$$

where the eigenfunctions $\phi_{n\alpha}$ and ϕ_{nE} of the decoupled set of equations (11) are normalized and δ normalized,

respectively. Hence Fano interference occurs in these situations.

In principle, it is possible to determine the Fano parameters Ω, Γ, and q from the wave functions ψ_n, $\psi_{n'}$, $\phi_{n\alpha}$, and $\phi_{n'E}$ using the equations in Ref. 1. This approach, however, does not yield the complete spectrum including all Landau levels and all exciton states. Therefore, we have chosen to perform a direct numerical calculation of the absorption spectrum in order to explicitly demonstrate the formation of Fano resonances and to examine the line shape. We have used the material parameters of GaAs, i.e., an exciton binding energy of $E_B = 4.9\,\mathrm{meV}$ and a reduced exciton mass of $m = 0.042\,m_0$ which is equal to the heavy-hole exciton mass obtained from literature data in Sec. II.

Figure 4(a) shows the optical susceptibility if Coulomb interaction is neglected, i.e., we assume $V_{nn'}(\zeta) \equiv 0$ for all n, n'. The magnetic field is 6 T, and a homogeneous broadening of $\hbar\eta = 0.02\,E_B$ is introduced. Since the Coulomb potential is neglected, the absorption spectrum coincides with the density of states, broadened by $\hbar\eta$.

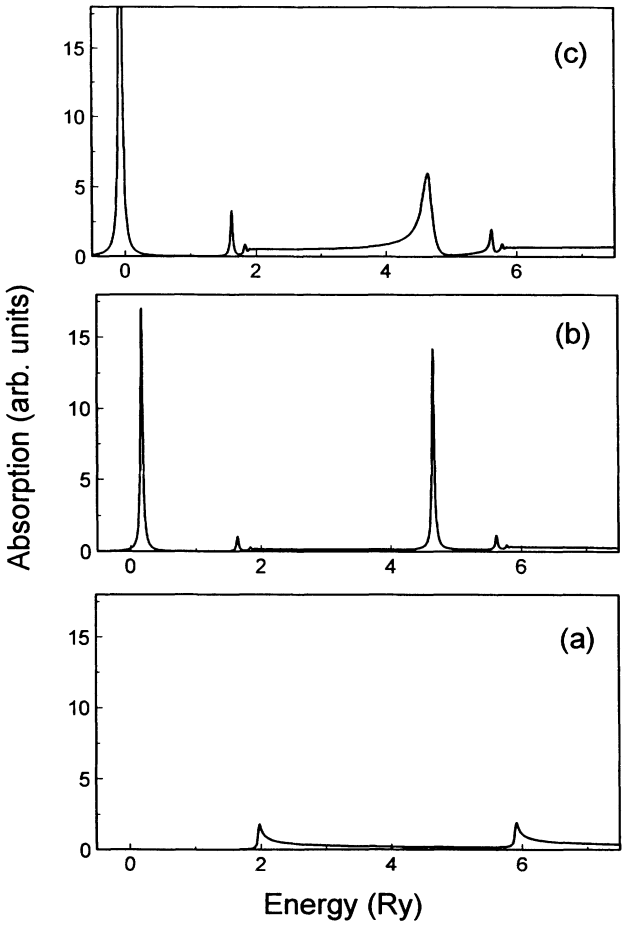

FIG. 4. Calculated optical absorption vs energy for a two-band semiconductor in a magnetic field of $B = 6$ T (homogeneous broadening $\hbar\eta = 0.02\,E_B$): (a) without Coulomb interaction, (b) with the diagonal part of the Coulomb potential, and (c) with the full Coulomb interaction.

In order to show the influence of the Coulomb potential, in the next step we consider the diagonal contributions (n=n') of the potential $V_{nn'}$. For this case, Eq. (11) decouples and can easily be solved. The result is shown in Fig. 4(b). Instead of the singularities of the density of states of each Landau level, now we find corresponding exciton series. The magnetoexcitons corresponding to the second (n=1) Landau level are degenerate to the continuum of the first (n=0) one. Yet we do not observe a Fano line shape since there is no coupling between the subbands. The spectrum is composed of a Lorentzian line on top of a flat continuum.

For the full Coulomb coupling Eq. (11) cannot be solved numerically. A straightforward generalization of the method used in Ref. 18 would imply a computational effort 10^9 times larger than for the two-dimensional problem. For this reason, no complete solution of Eq. (10), including continuum states, has been obtained until now. In order to circumvent these difficulties, we have discretized Eq. (10) on a uniform grid. This method has been well established in numerical mathematics for ten years. In physics, its efficiency has recently been demonstrated for electronic band structure calculations.[25]

The solution of the problem with the full Coulomb potential, which corresponds to Eq. (11) with all matrix elements $V_{nn'}$, is presented in Fig. 4(c). From the comparison of Figs. 4(c) and 4(b), it is obvious that the line shape of the magnetoexciton which is degenerate to continuum states drastically changes if the full Coulomb potential is taken into account. In contrast, the line shape of the magnetoexciton corresponding to the lowest Landau level remains Lorentzian independent whether the off-diagonal Coulomb matrix elements are included or not. Consequently, the change of the line shape of the higher-order magnetoexciton is the result of the coupling between the magnetoexciton and the continuum states. This coupling is obviously induced by the off-diagonal elements of the Coulomb potential. Since the lowest-order magnetoexciton does not overlap with continuum states, it is always an isolated eigenvalue and, therefore, shows a Lorentzian profile. As a general property of the Coulomb attraction, the continuum is enhanced in Fig. 4(c) compared to the free-particle case in Fig. 4(a) (Sommerfeld factor).

The asymmetric absorption profile, which is due to the Coulomb induced coupling between the higher-order magnetoexciton and the continuum, is a Fano resonance. In order to demonstrate this point unambiguously, we compare the line shapes of the lowest-order magnetoexciton and the higher-order magnetoexciton in Fig. 5 for the full Coulomb potential. Figure 5 is a close-up of Fig. 4(c), where both lines have been individually normalized but plotted on the same energy scale. The line shape of the magnetoexciton coupled to the continuum [Fig. 5(b)] shows the typical features of a Fano resonance. (i) The line shape is asymmetric. (ii) The width of the line is considerably larger than the introduced homogeneous broadening as can be seen from the comparison to the lowest-order magnetoexciton line in Fig. 5(a). The additional broadening stems from the coupling, in agree-

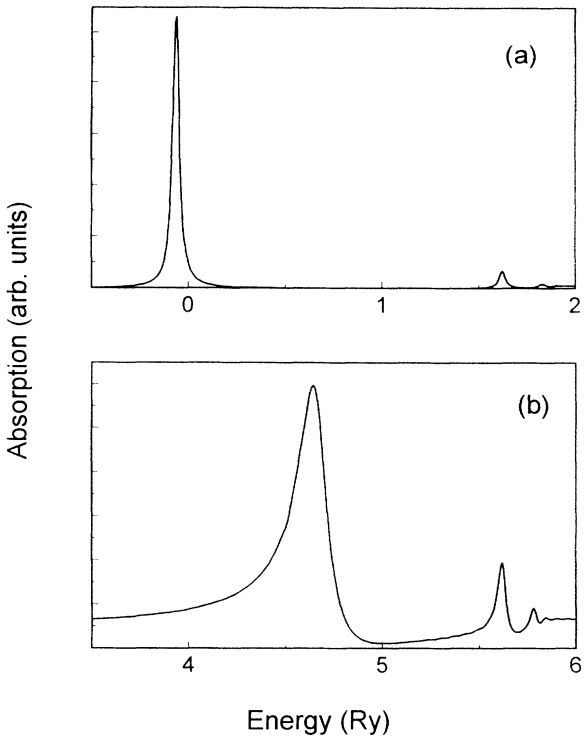

FIG. 5. Close-up of Fig. 4(c): (a) lowest-order magnetoexciton series, (b) higher-order magnetoexciton series.

ment with Fano's model.[1] (iii) There is a pronounced dip at the high-energy side of the absorption maximum. This dip extends well below the continuum level. The reason that the absorption minimum is slightly larger than zero is the finite homogeneous broadening. The differences between both types of line shapes are also observable for the excited exciton states. The above discussion unambiguously demonstrates that Fano resonances are formed and that the necessary coupling is induced by Coulomb interaction.

Figure 5 also shows that within the Rydberg series of Fano resonances the broadening and oscillator strength decrease uniformly with increasing quantum number so that the appearance of the line does not change much within the series.[1] In contrast, for a Lorentzian Rydberg series the broadening remains constant whereas the oscillator strength decreases considerably with increasing quantum number.

In order to verify that our theoretical model predicts the same magnetic field dependence of the absorption spectrum as observed experimentally, in Fig. 6 calculated spectra are shown for different magnetic fields $B = 0$, 6, and 12 T. This calculation has been done for the full Coulomb potential and a homogeneous linewidth of $\hbar\eta = 0.2\,E_B$. The spectra for $B = 6$ and 12 T have been numerically calculated. The calculation of the zero-field spectrum has been done analytically.[19]

The calculated absorption spectra for 6 and 12 T display Fano profiles in the continuum which are less pronounced compared to Fig. 4(c) due to the larger homogeneous broadening. As in the experiment, the height of the Fano resonance decreases with increasing energy. Of

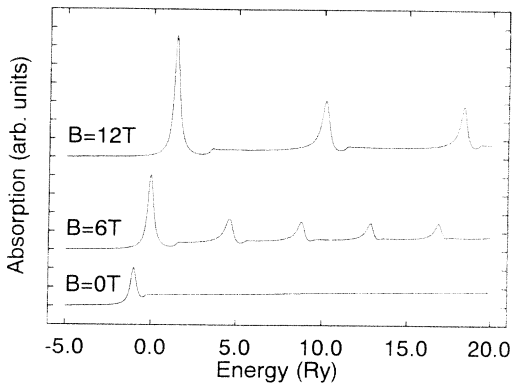

FIG. 6. Calculated optical absorption vs energy for magnetic fields $B = 0$, 6 and 12 T (homogeneous linewidth $\hbar\eta = 0.2\,E_B$).

course, the two-band model can only reproduce one series of resonances, whereas the experimental spectra show a light-hole and a heavy-hole series. Comparing the experimental heavy-hole data and the theoretical spectra, we find a good agreement in terms of the energy splitting between adjacent Fano resonances.

The calculated spectra confirm that this splitting in the high-energy region is about one cyclotron energy $\hbar\omega_c$ ($1.97\,E_B$ and $3.94\,E_B$ for 6 and 12 T, respectively) as it would be in the absence of Coulomb interaction. Furthermore, the calculated spectra reproduce the diamagnetic shift of the Lorentzian-shaped lowest-order magnetoexciton transition.

The comparison of the experimental and theoretical zero-field spectra shows that in the experiment the oscillator strength of the exciton is smaller compared to the continuum than in the calculated spectrum. This discrepancy has been found in all zero-field absorption experiments and calculations, and is not yet completely understood. This deviation between experiment and theory can also be observed in the Fano resonance spectra. Besides this deviation, the overall agreement between experiment and theory is excellent.

IV. CONCLUSION

We have presented an experimental and theoretical study of Fano interference in bulk GaAs under magnetic field. Fano interference in this system results from the coupling between higher-order magnetoexcitons and one-dimensional continuum states. In low-temperature linear absorption experiments, Fano interference manifests itself in the formation of asymmetric absorption lines with pronounced minima in the continuum part of the spectrum. These absorption profiles can be well described by Fano's model of a discrete state quantum mechanically coupled to a continuum of states.[1] This agreement unambiguously demonstrates that the observed absorp-

tion profiles are indeed Fano resonances. The Fano resonances can be traced back to the underlying light-hole and heavy-hole magnetoexcitons.

Theoretical calculations have been presented which show that Fano resonances are formed in bulk semiconductors if a magnetic field is applied, in agreement with the experimental findings. The theoretical treatment is based on the model of an isotropic two-band semiconductor in the effective-mass approximation. The model includes the magnetic field term and the Coulomb term. We have outlined how the linear absorption spectrum of this model semiconductor can be calculated. The numerical results reproduce the experimental observation of Fano resonances. Analytical and numerical calculations have shown that the Coulomb coupling of different Landau levels is the origin of the Fano resonances in the magnetoabsorption spectrum of bulk semiconductors.

ACKNOWLEDGMENTS

The authors wish to thank F. Bechstedt, S. Louie, S. Mukamel, P. Oswald, R. Ulbrich, and R. Zimmermann for helpful discussions. This work was supported by the Director, Office of Energy Research, Office of Basic Energy Sciences, Division of Material Sciences of the U.S. Department of Energy, under Contract No. DE-AC03-76SF00098. Furthermore, S. G. and U. S. want to thank the Deutsche Forschungsgemeinschaft for financial support.

[1] U. Fano, Phys. Rev. **124**, 1866 (1961).
[2] *Electron and Photon Interaction with Atoms,* edited by H. Kleinpoppen and M. R. C. McDowell (Plenum, New York, 1976).
[3] D. A. Broido and L. J. Sham, Phys. Rev. B **34**, 3917 (1986).
[4] H. Chu and Y.-C. Chang, Phys. Rev. B **39**, 10 861 (1989).
[5] K. Maschke, P. Thomas, and E. O. Göbel, Phys. Rev. Lett. **67**, 2646 (1991).
[6] D. Y. Oberli, G. Böhm, G. Weimann, and J. A. Brum, Phys. Rev. B **49**, 5757 (1994).
[7] J. J. Hopfield, P. J. Dean, and D. J. Thomas, Phys. Rev. **158**, 748 (1967).
[8] D. S. Chemla, A. Maruani, and E. Batifol, Phys. Rev. Lett. **42**, 1075 (1979).
[9] F. Bassani and A. Baldereschi, Surf. Sci. **37**, 304 (1973).
[10] Q. H. F. Vrehen, J. Phys. Chem. Solids **29**, 129 (1968).
[11] R. P. Seisyan, A. M. Abdullaev, and B. P. Zakharchenya, Sov. Phys. Semicond. **7**, 649 (1973) [Fiz. Tekh. Poluprov. **7**, 958 (1973)].
[12] S. B. Nam, D. C. Reynolds, C. W. Litton, R. J. Almassy, T. C. Collins, and C. M. Wolfe, Phys. Rev. B **13**, 761 (1976).
[13] W. Becker, B. Gerlach, T. Hornung, and R. G. Ulbrich, in *Proceedings of the 18th International Conference on the Physics of Semiconductors, Stokholm, Sweden, 1986,* edited by O. Engström (World Scientific, Singapore, 1987), p. 1713.
[14] F. H. Pollak and M. Cardona, Phys. Rev. **172**, 816 (1968).
[15] M. Jiang, H. Wang, R. Merlin, D. G. Steel, and M. Cardona, Phys. Rev. B **48**, 15 476 (1993).
[16] T. Rappen, G. Mohs, and M. Wegener, Appl. Phys. Lett. **63**, 1222 (1993).
[17] O. Madelung and W. Kress, in *Semiconductors. Physics of Group IV Elements and III-V Compounds,* edited by O. Madelung, M. Schulz, and H. Weiss, Landolt Börnstein, New Series, Group III, Vol. 17, Pt. a (Springer, Berlin, 1982), p. 158.
[18] C. Stafford, S. Schmitt-Rink, and W. Schäfer, Phys. Rev. B **41**, 10 000 (1990).
[19] R. J. Elliott, Phys. Rev. **108**, 1384 (1957).
[20] L. D. Landau and E. M. Lifshitz, *Course of Theoretical Physics* (Pergamon Press, New York, 1980), Vol. 9, p. 161.
[21] L. P. Gor'kov and I. E. Dzyaloshinskii, Sov. Phys. JETP **26**, 449 (1968) [Zh. Eksp. Teor. Fiz. **53**, 717 (1967)].
[22] J. Engbring and R. Zimmermann, Phys. Status Solidi B **172**, 733 (1992).
[23] K. Brunner, G. Abstreiter, M. Walter, G. Böhm, and G. Tränkle, Surf. Sci. **267**, 218 (1992).
[24] S. Glutsch and F. Bechstedt, Phys. Rev. B **47**, 6385 (1993).
[25] J. R. Chelikowsky, N. Troullier, and Y. Saad, Phys. Rev. Lett. **72**, 1240 (1994).